Simulation of 60-GHz microwave photonic filters based on serially coupled silicon microring resonators

Dengke Zhang (张登科), Xue Feng (冯 雪)*, and Yidong Huang (黄翊东)

State Key Laboratory of Integrated Optoelectronics, Department of Electronic Engineering, Tsinghua University, Beijing 100084, China

**Corresponding author: x-feng@tsinghua.edu.cn*

Received May 11, 2011; accepted July 14, 2011; posted online September 22, 2011

The microwave photonic filters (MPFs) based on serially coupled silicon microring resonators (MRRs) are theoretically analyzed for the application of 60-GHz millimeter wave wireless personal area networks. This is achieved by calculating the improvement of bit error ratio (BER). According to the simulation results, the requirement of signal-to-noise ratio (SNR) of the received data can be reduced by 14 dB for the same BER with and without MPFs. The performance of the MPF with five serially coupled microring structures is better than that of the MPF with a single microring, owing to the improvement of the shape factor.

OCIS codes: 130.3120, 070.6020.

doi: 10.3788/COL201210.021302.

In recent years, 60-GHz millimeter wave wireless personal area network (WPAN) has stimulated wide interest since it can be operated in unutilized spectrum. For this reason, WPAN is considered as the next generation network of short range wireless communication. The 60-GHz millimeter wave WPAN can be easily adopted to achieve multi-gigabit wireless network due to the huge and readily available spectrum allocation, as well as high frequency reuse ratio[1−3]. Due to high absorption of oxygen, 60-GHz millimeter wave signal would be seriously attenuated before reaching the receiver. Thus, it is critical to improve the signal-to-noise ratio (SNR) and bit error ratio (BER) for WPAN application. The most direct way to improve the SNR is to apply suitable millimeter wave filters. Since the traditional electrical microwave filters cannot operate well in high frequencies such as 60 GHz, microwave photonic filters (MPFs) provide a new approach in solving this obstacle.

MPFs can be used to process microwave (or even millimeter wave) signal in optical domain with beneficial characteristics such as low loss, wide bandwidth (BW), immunity to electromagnetic interference, and high speed operating frequency[4]. MPFs can be applied in numerous fields, including radar communications, satellite communications, and wireless communications. In the last decade, the megahertz (MHz) to gigahertz (GHz) operating frequency of MPFs has been achieved[5,6]. Several research groups have reported that the operating frequency can reach 10 GHz or higher[7,8]. However, this is still not high enough for 60-GHz millimeter wave filters. Aside from the operating frequency, MPFs are traditionally implemented with discrete photonic devices, such as fibers, $LiNbO_3$ modulators, wavelength division multiplexing (WDM) couplers, fiber gratings, and so on. Thus, MPF is not only a device but also a complicated subsystem. Recently, microring resonator (MRR) based MPFs fabricated on silicon-on-insulator (SOI) has attracted significant attention because of the simplicity with which they can be integrated with other optoelectronic integrated circuit (IC) components[9] and the facility with which they can reach a higher operating frequency[10]. Pile *et al.* investigated the operation principle of MRR-MPF in theory, and the noise and distortion performance were analyzed as well[11]. Rasras *et al.* demonstrated a notch MRR-MPF with 10-GHz operating frequency[12], and Palací *et al.* realized 10–80 GHz band-pass MPFs based on signal MRR[10]. However, there are no reported studies on the performance of MRR-MPFs as applied in wireless communication.

In this letter, MPFs based on silicon MRRs are designed for the application in 60-GHz millimeter wave WPAN. Improvement on the behavior of BER with serially coupled rings is analyzed. After clarifying the general operation of MPFs based on serially coupled MRRs with various ring numbers in detail, two MRR-MPFs are designed and demonstrated with single and five serially coupled MRRs. Furthermore, the simulated BER results for the transmission in 60-GHz millimeter wave WPAN are presented and discussed.

Figure 1(a) depicts the scheme of a typical MPF with intensity modulation and direct detection. The continuous-wave (CW) laser source $e_c(t)$ is modulated by the microwave input signal $v_i(t)$ via the dual-drive Mach-Zehnder modulator (MZM). The modulated light $e_m(t)$ passes through the optical filter and is received

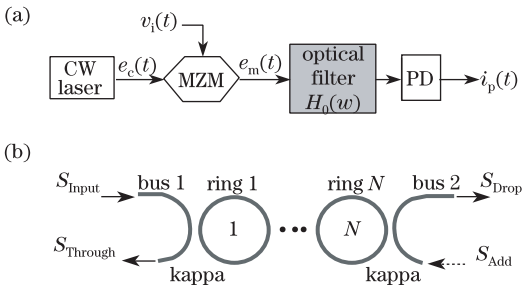

Fig. 1. (a) Schematic of MPF and (b) optical filter of NR2B.

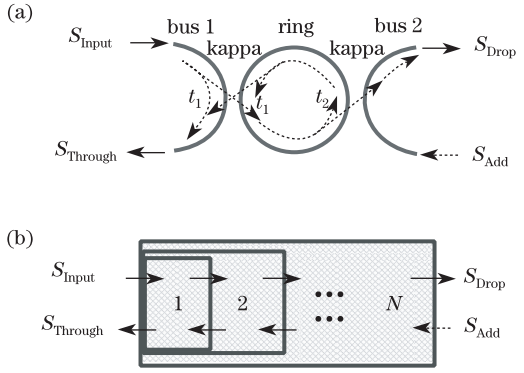

Fig. 2. (a) Basic 1R2B filter and (b) model of analysis for NR2B using iterative method.

by a photodetector (PD), and finally transformed into electrical signal $i_{\text{p}}(t)$. The optical filter in Fig. 1(a) is considered as serially coupled MRRs as shown in Fig. 1(b).

Firstly, the optical filter response of serially coupled MRRs, which contain N rings and two buses (NR2B), is obtained based on the response of single MRR according to the procedure composed of the following three steps:

(1) The basic optical filter response of single MRR is analyzed with Fabry-Perot (FP) resonator model as shown in Fig. 2(a). The optical transfer function $H^1_{\text{O\_I}\to\text{T}}(\omega)$ of "Input" port to "Through" port for 1R2B-MRR can be deduced as

$$H^1_{\text{O\_I}\to\text{T}}(\omega)=\frac{S_{\text{Through}}}{S_{\text{Input}}}=\frac{t_1-t_2a\cdot\mathrm{e}^{-\mathrm{j}(\omega n_{\text{eff}}L/c)}}{1-t_1t_2a\cdot\mathrm{e}^{-\mathrm{j}(\omega n_{\text{eff}}L/c)}}, \quad (1a)$$

and the response $H^1_{\text{O\_I}\to\text{D}}(\omega)$ of "Input" port to "Drop" port is

$$H^1_{\text{O\_I}\to\text{D}}(\omega)=\frac{S_{\text{Drop}}}{S_{\text{Input}}}=-\frac{\kappa_1\kappa_2\sqrt{a}\cdot\mathrm{e}^{-\mathrm{j}(\omega n_{\text{eff}}L/c)/2}}{1-t_1t_2a\cdot\mathrm{e}^{-\mathrm{j}(\omega n_{\text{eff}}L/c)}}, \quad (1b)$$

where ω is optical frequency, c is the speed of light in vacuum, L is ring circumference, a is the single-pass amplitude transmission, n_{eff} is the effective refractive index of the waveguide, and t_n and κ_n represent self- and cross-amplitude coupling coefficients between the nth bus and the ring, respectively, which should satisfy $t_n^2+\kappa_n^2=1$. When the light is injected from the "Add" port, the corresponding transfer functions $H^1_{\text{O\_A}\to\text{D}}(\omega)$ and $H^1_{\text{O\_A}\to\text{T}}(\omega)$ can be deduced similarly.

(2) The coupling of serially coupled MRRs can be solved using the iteration method. As shown in Fig. 2(b), the transmission and reflection coefficients of the first MRR can be seen as the cross- and self-coupling coefficients at input port of the second MRR. Thus, the response of 2R2B-MRR can be obtained by the same method in step (1). The same procedure can be iterated until all of the MRRs are calculated. Subsequently, the optical responses $H^n_{\text{O\_I}\to\text{T}}(\omega)$ and $H^n_{\text{O\_I}\to\text{D}}(\omega)$ for n rings ($n\geqslant 2$) can be expressed as

$$H^n_{\text{O\_I}\to\text{T}}(\omega)=H^{n-1}_{\text{O\_I}\to\text{T}}(\omega)+\frac{H^{n-1}_{\text{O\_I}\to\text{D}}(\omega)H^{n-1}_{\text{O\_A}\to\text{T}}(\omega)t_{n+1}a\cdot\mathrm{e}^{-\mathrm{j}(\omega n_{\text{eff}}L/c)}}{1-H^{n-1}_{\text{O\_A}\to\text{D}}(\omega)t_{n+1}a\cdot\mathrm{e}^{-\mathrm{j}(\omega n_{\text{eff}}L/c)}}, \quad (2a)$$

$$H^n_{\text{O\_I}\to\text{D}}(\omega)=\frac{jH^{n-1}_{\text{O\_I}\to\text{D}}(\omega)\kappa_{n+1}\sqrt{a}\cdot\mathrm{e}^{-\mathrm{j}(\omega n_{\text{eff}}L/c)/2}}{1-H^{n-1}_{\text{O\_A}\to\text{D}}(\omega)t_{n+1}a\cdot\mathrm{e}^{-\mathrm{j}(\omega n_{\text{eff}}L/c)}}. \quad (2b)$$

In this letter, the focus is on the "Drop" port output. The response of $H^n_{\text{O\_I}\to\text{D}}(\omega)$ is adopted in MRR-MPF simulation since a band-pass filter is required for noise filtering.

(3) The rational function responses of serially coupled MRRs are synthesized with the traditional insertion loss method. For NR2B MRRs, the spectrum is determined by the vector of coupling coefficients $\mathbf{C}^N=[\kappa_1,\cdots,\kappa_{N+1}]$ of filters. Maximally flat responses can be obtained as shown by Little *et al.*[13]. Based on this, the calculated results of the coefficient vector are summarized in Table 1 for 1R2B, 3R2B, and 5R2B MRRs.

With the procedure described above, the maximally flat optical response of NR2B-MRR can be obtained and consequently, the general performance of MRR-MPFs can be derived.

Table 1. Relationships of Coupling Coefficients

Type	$\mathbf{C}^N$	Maximally Flat	Used in Simulation
1R2B	$\mathbf{C}^1$	$\kappa_1=\kappa_2$	$\kappa_1=\kappa_2=0.276$
3R2B	$\mathbf{C}^3$	$\kappa_1=\kappa_4$ $\kappa_2^2=\kappa_3^2=0.125\kappa_1^4$	
5R2B	$\mathbf{C}^5$	$\kappa_1=\kappa_6$ $\kappa_2^2=\kappa_5^2=0.0955\kappa_1^4$ $\kappa_3^2=\kappa_4^2=0.0295\kappa_1^4$	$\kappa_1=\kappa_6=0.784$ $\kappa_2=\kappa_5=0.190$ $\kappa_3=\kappa_4=0.106$

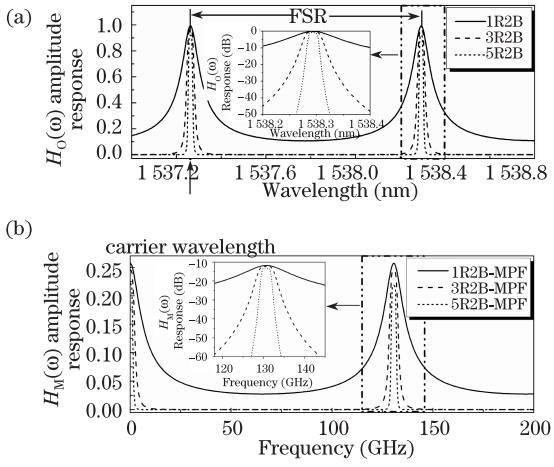

Fig. 3. (a) Typical optical spectra of 1R2B, 3R2B, and 5R2B MRRs and (b) corresponding microwave spectra of MPFs based on 1R2B, 3R2B, and 5R2B MRRs. The insets show the corresponding spectra in rectangular boxes, in decibels.

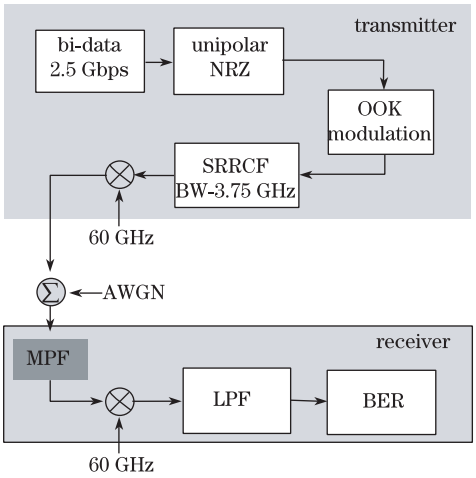

Fig. 4. Schematic of simulation procedure.

In order to ensure the linear response of MPF, the modulation depth $m = \pi v_{\rm m}/V_\pi$ should satisfy $m \ll 1$, where $v_{\rm m}$ is the amplitude of microwave signal and V_π is the half-wave voltage of electro-optic modulator. According to the result in Ref. [11], when the MPF operates with symmetry carrier placement, a microwave transfer function $H_{\rm M}(\omega_{\rm m})$ for double-sideband plus carrier (DSB+C) modulation can be given as

$$H_{\rm M}(\omega_{\rm m}) \approx \frac{{\rm j}2\Re P_{\rm c}}{v_{\rm m}} {\rm J}_0(m){\rm J}_1(m)H_{\rm o}(\omega_{\rm c})H_{\rm o}(\omega_{\rm c}+\omega_{\rm m}), \quad (3)$$

where $\omega_{\rm c}$ and $\omega_{\rm m}$ are the optical carrier and microwave signal frequency, respectively, $\Re$ is the responsivity of an ideal photodetector, $P_{\rm c}$ is the input laser power, $J_n(\cdot)$ is the nth-order Bessel function of the first kind, and $H_{\rm o}(\cdot)$ is the transfer function of optical filter, which is the "Input" port to "Drop" port response of serially coupled MRRs as shown in Eq. (2b).

Using Eqs. (1)–(3), the typical optical spectra of 1R2B, 3R2B, and 5R2B MRRs and corresponding microwave spectra of MPFs are calculated. Results are shown in Fig. 3.

Based on Eq. (3) and the results shown in Fig. 3, the free spectral range (FSR) and BW of microwave spectra are equal to those of optical spectra. Thus, when the wavelength of optical carrier lies in one of resonating wavelengths of MRRs, the center frequency of the first passband of MPFs should be equal to that of the FSR shown in Fig. 3(a). The insets of Fig. 3 show the corresponding spectra in rectangular boxes, in decibels. Shape factor (SF) of MPF spectrum, defined as ${\rm BW}_{-3\ {\rm dB}}/{\rm BW}_{-20\ {\rm dB}}$, increased with the increase in the number of rings. In other words, more noise could be filtered with the MPFs based on 5R2B MRRs. For this kind of MPFs, the BW is related to the intrinsic losses of MRRs and coupling coefficients. Thus, the BW has a lower limit because of the intrinsic losses of MRRs. However, larger BW can be achieved by increasing the coupling coefficients.

To investigate the improvement of SNR and BER for 60-GHz millimeter wave WPAN application, two MPFs based on 1R2B and 5R2B MRRs are adopted and compared. As shown in Fig. 4, the calculated wireless communication system is considered as a 2.5-Gbps baseband signal carried by 60-GHz millimeter wave. Unipolar nonreturn-to-zero (NRZ) data signal is modulated to OOK signal and pulse shaping is realized by square-root raised cosine filter (SRRCF) with roll-off factor of 0.5. This leads to the extension of BW to 3.75 GHz. In the simulation, the noise in the transmission channel is introduced by the complex environment of wireless communications, and is considered as additive white Gaussian noise (AWGN). Shot and thermal noises generated in the receiver are not considered since the considered MPFs are not capable of dealing with these noises. In the receiver, the signal is demodulated to baseband data with a 50-GHz low pass filter (LPF) and sent to error code tester for BER testing. In our simulation, pseudorandom bit sequence with a length of 50 is tested 50 times. For comparison, both cases of with and without MPFs at the front of receiver are calculated as well as the case of using matched filter (MF).

In our simulation, MRRs are assumed to be fabricated on SOI, where the cross-section of silicon waveguide is 220×500 (nm) and the propagation loss of waveguide is 2 dB/cm. The circumference of microring is designed as 1.385 mm to achieve FSR of 60 GHz. The carrier wavelength of 1 550.33 nm is one of the resonating wavelengths of MRRs and the coefficient vector of 1R2B and that of 5R2B for BW of 3.75 GHz can be found in the fourth column of Table 1. To maintain the center frequency of the spectra, high stability of carrier wavelength is required. The other parameters of our designed MPFs for simulation are $P_{\rm c} = 10$ mW, $\Re = 0.5$ A/W, $V_\pi = 1$ V, and $v_{\rm m} = 0.05$ V.

Figure 5 shows the spectra of the two designed MPFs with center frequency of 60 GHz and BW of 3.75 GHz. The calculated SFs are also shown in the inset. The SFs for 1R2B, 5R2B MRR-MPF, and MF are 0.09, 0.51, and 0.69, respectively. The SF of 5R2B MRR-MPF is closer to that of MF. The results of the BER test with the application of the two MPFs on the 60-GHz millimeter wave WPAN system are shown in Fig. 6. Several representative eye diagrams of BER test are also shown in the insets. Apparently, the BERs can be reduced dramatically by applying MPFs. For the case without MPFs, the BER is approximately 10^{-9} with SNR of 15 dB. The bit-error-free communication can be achieved with SNR higher than 17 dB for this case. When the

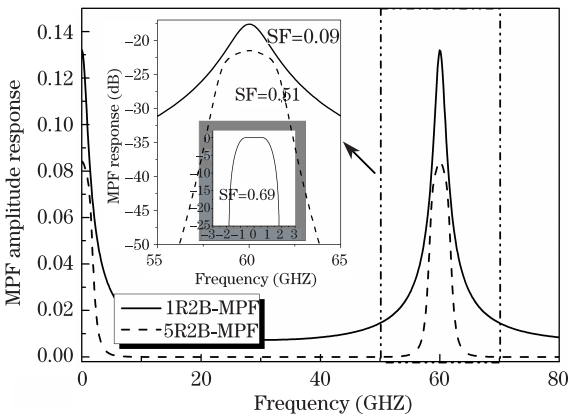

Fig. 5. Microwave spectra of two designed MPFs based on 1R2B and 5R2B. Inset shows the SFs of the two MPFs. The gray inset presents the spectrum of the MF.

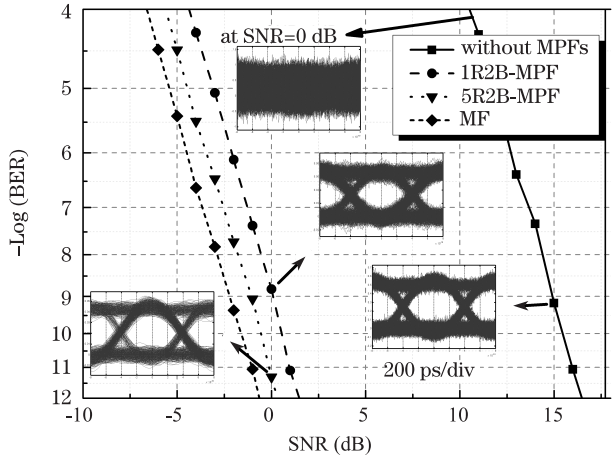

Fig. 6. Behavior of BER versus SNR of received data using MPFs based on 1R2B and 5R2B MRRs, no MPFs, and MF. Insets show four representative eye diagrams of BER test.

SNR is reduced to 0 dB, BER can be reduced from 10^{-1} to lower than 10^{-9} with MRR-MPFs base on 1R2B and 5R2B structures. This indicates that the required SNR of the received data can be reduced by 14 dB or higher to achieve the same BER in comparison with those without MPFs. 5R2B MRR-MPF can achieve better BER compared with 1R2B because SF of 5R2B MRR is considerably closer to that of MF as mentioned above. Thus, the SNR is improved remarkably.

In conclusion, the MPFs based on the serially coupled MRRs are theoretically analyzed toward application in 60-GHz millimeter wave WPAN. The SNR and BER are improved dramatically when using these MPFs. Two MRR-MPFs based on 1R2B and 5R2B are designed and adopted on the wireless communication with 2.5-Gbps baseband signal carried by 60-GHz millimeter wave. The requirement for SNR of the received data can be reduced by 14 dB for the same BER, and the performance of the 5R2B MRR-MPF is better than that of 1R2B because better SF could be achieved. However, this improvement is not remarkable because most noise is located outside of BW. Nevertheless, higher SF leads to smaller signal distortion. As the optoelectronic integration technology matures, MPFs based on the serially coupled MRRs are expected to be recognized and applied to wireless communication systems. In this connection, related work is ongoing.

This work was supported by the National "973" Program of China (No. 2007CB307004), the National Natural Science Foundation of China (No. 60877023), and the Project of National Information Control Laboratory. The authors would like to thank W. Zhang, F. Liu, K. Cui, and G. Zhang for their valuable insights and helpful comments.

References

1. A. Stöhr, A. Akrout, R. Buß, B. Charbonnier, F. van Dijk, A. Enard, S. Fedderwitz, D. Jäger, M. Huchard, F. Lecoche, J. Marti, R. Sambaraju, A. Steffan, A. Umbach, and M. Weiß, J. Opt. Netw. **8,** 471 (2009).
2. Z. Cao, J. Yu, Q. Tang, G. Zeng, and L. Chen, Chin. Opt. Lett. **8,** 1024 (2010).
3. Q. Tang, L. Chen, J. Xiao, and Z. Cao, Chin. Opt. Lett. **9,** 050601 (2011).
4. J. Capmany, B. Ortega, and D. Pastor, J. Lightwave Technol. **24,** 201 (2006).
5. D. B. Hunter and R. A. Minasian, IEEE Photon. Technol. Lett. **11,** 874 (2002).
6. J. Palací, P. Pérez-Millán, G. E. Villanueva, J. L. Cruz, M. V. Andrés, J. Martí, and B. Vidal, IEEE Photon. Technol. Lett. **22,** 1467 (2010).
7. M. Popov, P. Fonjallaz, and O. Gunnarsson, IEEE Photon. Technol. Lett. **17,** 663 (2005).
8. J. Mora, B. Ortega, A. Diez, J. L. Cruz, M. V. Andres, J. Capmany, and D. Pastor, J. Lightwave Technol. **24,** 2500 (2006).
9. A. Barkai, Y. Chetrit, O. Cohen, R. Cohen, N. Elek, E. Ginsburg, S. Litski, A. Michaeli, O. Raday, D. Rubin, G. Sarid, N. Izhaky, M. Morse, O. Dosunmu, A. Liu, L. Liao, H. Rong, Y. Kuo, S. Xu, D. Alduino, J. Tseng, H. Liu, and M. Paniccia, J. Opt. Netw. **6,** 25 (2007).
10. J. Palací, G. E. Villanueva, J. V. Galán, J. Martí, and B. Vidal, IEEE Photon. Technol. Lett. **22,** 1276 (2010).
11. B. C. Pile and G. W. Taylor, IEEE Trans. Microw. Theor. Technol. **57,** 487 (2009).
12. M. S. Rasras, K. Tu, D. M. Gill, Y. Chen, A. E. White, S. S. Patel, A. Pomerene, D. Carothers, J. Beattie, M. Beals, J. Michel, and L. C. Kimerling, J. Lightwave Technol. **27,** 2105 (2009).
13. B. E. Little, S. T. Chu, H. A. Haus, J. Foresi, and J.-P. Laine, J. Lightwave Technol. **15,** 998 (1997).